

Polyoxometalate-Induced Efficient Recycling of Waste Polyester Plastics into Metal–Organic Frameworks

Yong-Jun Chen^{1†}, Xianqiang Huang^{2†}, Yifa Chen^{1*}, Yi-Rong Wang¹, Haichao Zhang², Chun-Xia Li², Lei Zhang¹, Hongjing Zhu¹, Ruxin Yang¹, Yu-He Kan³, Shun-Li Li¹ & Ya-Qian Lan^{1*}

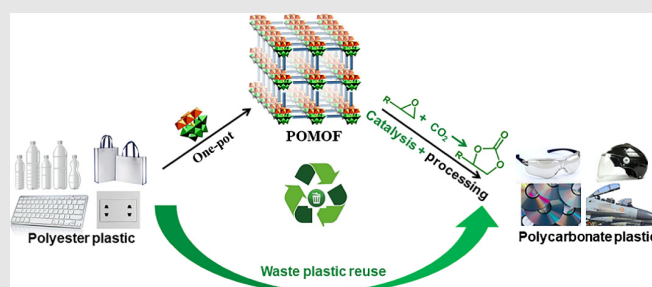
¹Jiangsu Collaborative Innovation Centre of Biomedical Functional Materials, Jiangsu Key Laboratory of New Power Batteries, School of Chemistry and Materials Science, Nanjing Normal University, Nanjing 210023 (China), ²Provincial Key Laboratory of Chemical Energy Storage and Novel Cell Technology, School of Chemistry & Chemical Engineering, Liaocheng University, Liaocheng, Shandong 252059 (China), ³Jiangsu Province Key Laboratory for Chemistry of Low-Dimensional Materials, School of Chemistry and Chemical Engineering, Huaiyin Normal University, Huai'an 223300 (China)

*Corresponding authors: chyf927821@163.com; yqlan@njnu.edu.cn; [†]These authors contributed equally.

Cite this: *CCS Chem.* **2019**, *1*, 561–570

Polyester plastics such as poly(ethylene terephthalate) (PET) are utilized commonly in everyday life, yet only a small portion of these plastics are recycled, and typically, the recycling procedures face energy or pollution problems. Accordingly, methods that could convert waste polyester plastics into value-added products like metal-organic frameworks (MOFs) are desirable. For the first time, we report a general and versatile polyoxometalate-based plastic hydrolysis protocol for one-pot syntheses of polyoxometalate-based metal-organic frameworks (POMOFs). We show that this protocol could be applied to diverse kinds of plastics [i.e., PET and poly(butylene terephthalate)] and various polyoxometalate systems (i.e., Ni_6PW_9 , $\text{Zn}_4\text{PMo}_{12}$, and V_6S) to generate POMOFs (i.e., Ni-POMOF, Z-POMOF, and VMOP-11) with ~100% hydrolysis efficiency. Besides, this method could be easily scaled up, and the large-scale POMOFs obtained could efficiently catalyze the

syntheses of cyclic carbonates in simulated flue gas from a coal-fired power plant. Thus, our approach of polyester plastic hydrolysis into valuable, eco-friendly, and biodegradable POMOFs sheds light on the development of novel techniques in waste-plastic recycling.



Keywords: polyester plastic, polyoxometalate, metal-organic frameworks, high hydrolysis efficiency, plastic reuse

Introduction

Waste-plastics generation has become a global issue of concern.¹ In 2018, the total consumption of plastics reached ~8 billion tons, and about 70% of them were discarded worldwide.² Most of the disposed waste had

high durability and resistant to biodegradation, and thus, could stay in the environment for hundreds of years, and ultimately, create a severe global environmental crisis.³ Moreover, despite the tremendous amount of plastics discarded, only about 9% of them are recycled.⁴ It has been estimated that between now and 2050, the

estimated amount of plastics expected to be generated would be as large as 34 billion tons, and the accumulated waste would reach 33 billion tons.⁵ Hence, increased in more and more waste plastics over time would likely cause terrifying ecological pollution, with an unfavorable economic challenge. Therefore, efficient plastic waste recycling approaches are highly necessary.

Polyester plastics such as poly(ethylene terephthalate) (PET) or poly(butylene terephthalate) (PBT) with properties like high strength, durability, and safety have been utilized commonly in our daily lives.^{6,7} For example, PET could be applied in the fabrication of textile fibers or bottles, and PBT is used typically as electrical plastics. In 2017, the reported annual production of PET and PBT were ~300 and 7.5 million tons worldwide, respectively; yet, only as low as ~7% PET and 5% PBT were recycled, which calls for a high demand of recycling processes to support this global challenge. However, recycling procedures generally, face energy or pollution problems. For instance, the recycling of PET involves methods like primary recycling (e.g., preconsumer industrial scrap and salvage), secondary recycling (e.g., physical reprocessing), and tertiary recycling (e.g., chemical recycling).⁸ Among them, chemical recycling processes such as hydrolysis are highly crucial for PET recycling, since they result in achieving beneficial industrial raw materials like terephthalic acid (H_2BDC) used as metal-organic frameworks for heterogeneous catalysis, fabrication of powders and water-soluble coatings.^{9,10} However, there are still drawbacks like the use of large amount of acid (e.g., HF or HCl, etc.) or base (e.g., NaOH or KOH, etc.),

high temperature (200–250 °C) or pressure (1.4–2 MPa), as well as long-time periods required to complete depolymerization.¹¹ Besides, these stringent reaction conditions, many complicated steps are involved, thus, imposing large energy consumption and enormous environmental threats. Except for PET, other polyester plastics such as PBT also face similar problems;¹² hence, strategies that could efficiently hydrolyze polyester plastics and further convert them into economically valuable products without incurring additional pollution concerns are long-sought-after.

Metal-organic frameworks (MOFs) are a class of porous crystalline materials constructed from metal ions and organic linkers, which have been investigated widely.^{13–15} Due to their crystallinity, porosity, and malleability, MOFs hold great promise in many applications such as gas storage/separation, sensing, and catalysis.^{16–19} Polyoxometalate-based metal-organic frameworks (POMOFs), a unique class of MOFs, integrate the functionality of both polyoxometalates (POMs) and MOFs, presenting many essential and attractive properties.^{20–22} The assembly of stable and functional cluster-based POMOFs is a significant pursuit in modern crystal engineering, chemistry, and materials science.²³ Concerning the construction units of waste, polyester plastics are organic ligands like H_2BDC (about 85 wt % in PET). We envisioned that it would be of tremendous economic value to produce high-value-added products like MOFs or POMOFs from waste polyester plastics.²⁴

To date, some works have reported encouraging results. For example, in PET research, one of the

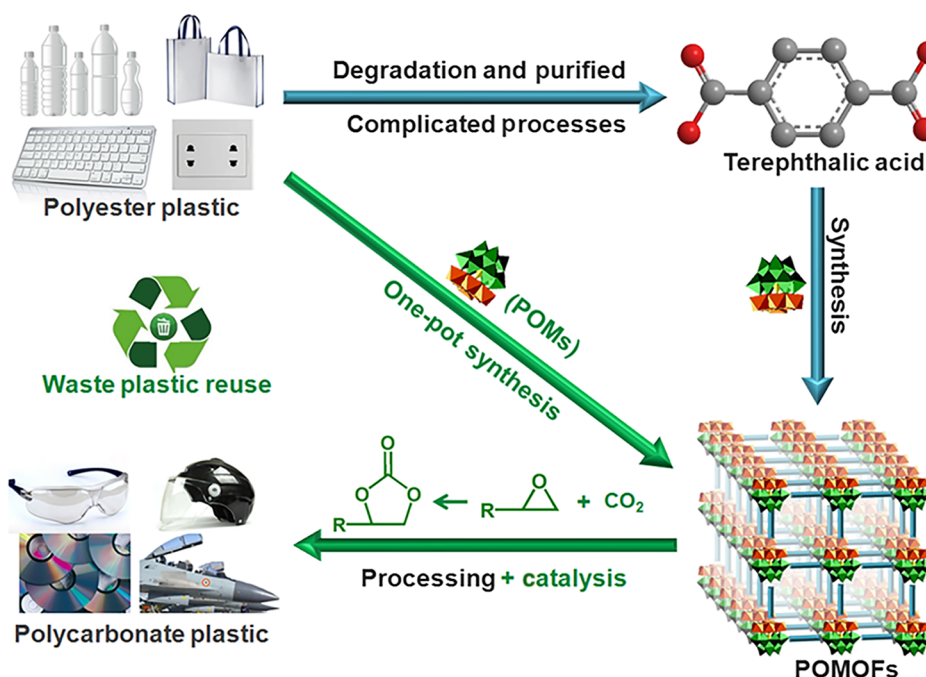


Figure 1 | Schematic illustration of the one-pot POM-induced polyester plastic hydrolysis reaction.

advances has been an attempt to convert PET into MOFs by applying two-step methods involving conversion of waste PET into H_2BDC , which is, in turn, used for the synthesis of MOFs like Cr-MOFs, MIL-47, or UiO-66.²⁵⁻²⁸ However, the separated depolymerization and synthesis processes have been shown to be energy- as well as time-consuming. To bypass these obstacles, other investigators have made use of direct conversion of PET into trivalent MOFs (e.g., MIL-47, MIL-53, and MIL-101, etc.) or pillared-paddlewheel MOFs [e.g., $\text{M}_2(\text{BDC})_2(\text{DABCO})$] with the addition of HF, HCl, formic acid, or NaOH, under hydrothermal conditions.^{24,29,30} Despite these inspiring results, there are still drawbacks for these direct conversion methods, which are as follows: (1) Low PET conversion efficiency, mostly lower than 80%. (2) The usage of large amounts of acids or bases, like recycling and other treatments, might face energy consumption or environmental problems. (3) The types of MOFs conversions are limited, while other MOF types like POMOFs remain unexplored. (4) The exploration of waste conversions is only on PET; other polyester plastics like PBT

conversions are rarely reported. Therefore, in our study design, we considered that a versatile approach that could directly and efficiently convert various polyester plastics into multifunctional MOFs like POMOFs, with reduced usage of acid or base or their entire prevention in the reaction procedures for highly desirable outcomes.

Herein, our approach is the first to report a type of POM-based plastic hydrolysis protocol for the one-pot syntheses of POMOFs (Figure 1). This protocol could be applied to diverse types of polyester plastics (i.e., PET and PBT), various POM systems [e.g., polytungstate (Ni_6PW_9), polyoxomolybdate ($\text{Zn}_4\text{PMo}_{12}$), and polyoxovanadate (V_6S)] to generate POMOFs (i.e., Ni-POMOF, Z-POMOF, and VMOP-11) with close to 100% to 100% hydrolysis efficiency (Figure 2a). POMOFs were obtained from the environmental-friendly method, which could efficiently catalyze the synthesis of a series of cyclic carbonate compounds (precursors for polycarbonate plastics after further processing) to achieve the conversion from one type of plastic to another (Figure 1). Moreover, this versatile approach could be easily scaled up to

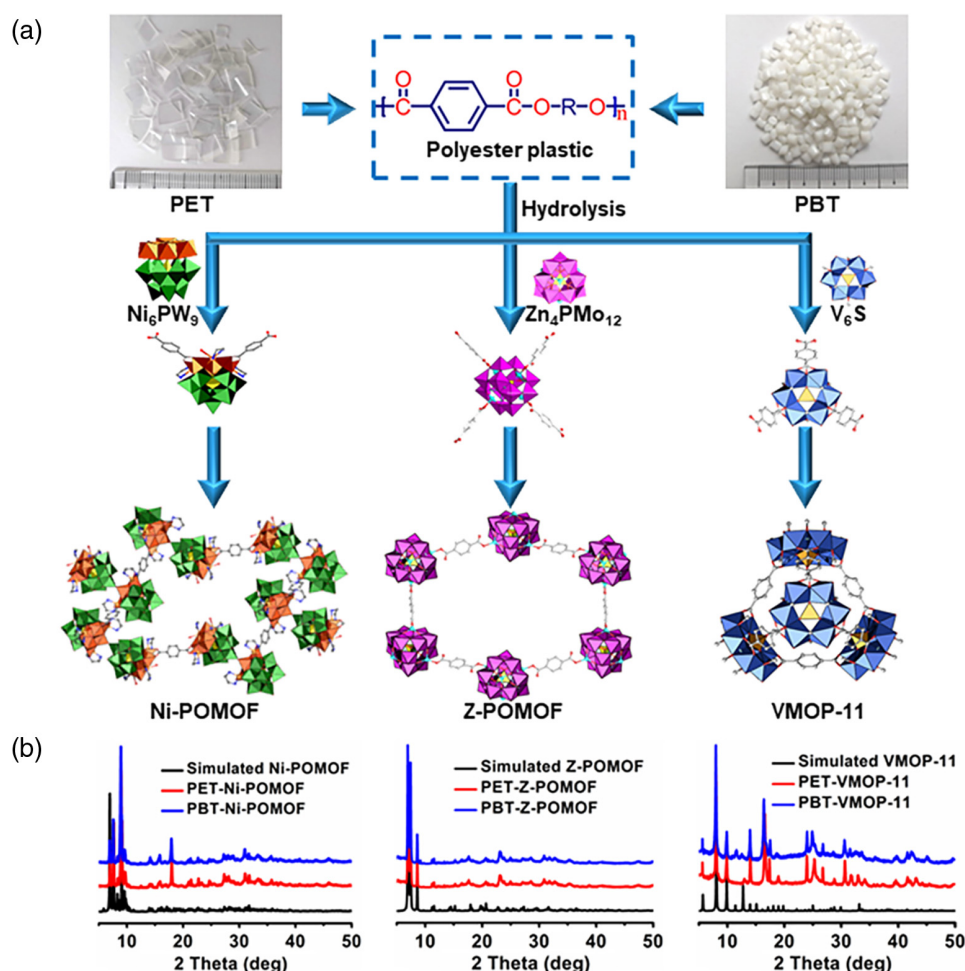


Figure 2 | Schematic illustration of the conversion and characterization of polyester plastics. (a) Conversion of polyester plastics into various POMOFs. (b) PXRD patterns of POMOFs obtained from PET and PBT conversions.

15 times successive expansion using the original set conditions, thereby, rendering it promising in industrial-scale production.

Experimental Methods

Preparation of waste plastics

Clear PET plastic ($M_n = 4.92 \times 10^4$ g·mol⁻¹ and $M_w = 8.36 \times 10^4$ g·mol⁻¹) bottles were collected from domestic waste as the raw materials. After removal of the caps, rings, and labels, the cleaned bottle bodies were cut into small flakes (about $5.5 \times 4.0 \times 0.2$ mm) with scissors, which were used for the experiments. The PBT white particles with dimensions of about $3.0 \times 3.0 \times 2.0$ mm ($M_n = 3.27 \times 10^4$ g·mol⁻¹ and $M_w = 4.03 \times 10^4$ g·mol⁻¹) were purchased from commercial sources (Shanghai Huahe composite material Co., Shanghai, China). All the plastic samples were washed with water and ethanol several times and dried under vacuum for further usage.

Syntheses of PET-Ni-POMOF and PBT-Ni-POMOF

A mixture of $\text{Na}_3[\text{A-}\alpha\text{-PW}_9\text{O}_{34}] \cdot n\text{H}_2\text{O}$ (0.15 g, 0.06 mmol) and $\text{NiCl}_2 \cdot 6\text{H}_2\text{O}$ (0.40 g, 1.68 mmol) was added into 0.5 M sodium acetate buffer (pH = 4.8, 5 mL) and stirred for 5 min, forming a clear green solution. Then ethylenediamine (0.15 mL) was added dropwise into the solution with continuous stirring. PET (0.10 g, 0.52 mmol) was also added into the mixture and stirred for 120 min. After that, the mixed solution was sealed in a 15 mL Teflon-lined stainless steel autoclave tube and heated at 180 °C for 72 h. After cooling to room temperature, the remaining PET was separated by hand-picking and flotation, and the green powder obtained was washed three times each with water and ethanol. Powder X-ray diffraction (PXRD) technique was used to estimate the phase of PET-Ni-POMOF in the reaction. The Fourier-transform infrared (FT-IR) peaks were used to identify molecular components of the PET-Ni-POMOF structure listed as follows: FT-IR (KBr, cm⁻¹) 3650 (w), 1620 (s), 1500 (w), 1310 (s), 1190 (w), 1125 (w), 1036 (m), 939 (w), 810 (s), 753 (s), 600 (s), 560 (w), 520 (w), 500 (s), 450 (m). Elemental Anal. Ratios Calcd (%) for $\text{C}_{26}\text{H}_{89}\text{N}_{14}\text{Ni}_{13}\text{O}_{90}\text{P}_2\text{W}_{18}$: C, 5.05; H, 1.52; O, 23.85; N, 3.21; P, 0.9; Ni, 12.08; W, 53.01. Calcd found (%): C, 4.88; H, 1.89; O, 23.91; N, 3.02; P, 1.04; Ni, 12.13; W, 52.16. Inductively coupled plasma (ICP) and elemental analyses were used to calculate the formula of PET-Ni-POMOF.

The preparation process of PBT-Ni-POMOF was similar to that of PET-Ni-POMOF except that PET (0.10 g, 0.52 mmol) was replaced by PBT (0.10 g, 0.45 mmol). PXRD and FT-IR were employed to determine the hydrolysis efficiency and to identify the molecular components of PBT-Ni-POMOF, as described above.

Syntheses of PET-Z-POMOF and PBT-Z-POMOF

A mixture of H_3PO_3 (0.02 g, 0.25 mmol); ZnCl_2 (0.14 g, 1 mmol); $(\text{NH}_4)_2\text{Mo}_7\text{O}_{24} \cdot 4\text{H}_2\text{O}$ (0.62 g, 3.50 mmol); molybdenum powder (0.06 g, 0.62 mmol); PET (0.064 g, 0.32 mmol); and tetrabutylammonium hydroxide solution (640 μL , 10 wt % in water) was added into 8 mL H_2O and stirred for 15 min. After the pH was adjusted to ~5 (small amount of hydrochloric acid was used for the essential synthesis of POM), the solution was sealed in a 15 mL Teflon-lined stainless steel autoclave tubes and heated at 180 °C for 72 h. After cooling to room temperature, the remaining PET was separated by hand-picking and flotation, and the dark red crystals obtained were washed three times with water and ethanol. PXRD and FT-IR were employed to determine the hydrolysis efficiency of PET derivative, PET-Z-POMOF, in the reaction. The FT-IR peaks are listed as follows (KBr, cm⁻¹): 2450 (w), 2210 (w), 1670 (w), 1460 (s), 1250 (w), 1036 (m), 950 (s), 730 (m), 700 (w), 610 (w), 550 (w). Anal. Calcd (%) for $\text{C}_{64}\text{H}_{124}\text{O}_{50}\text{N}_3\text{Zn}_4\text{PMo}_{12}$: C, 24.36; H, 3.79; O, 24.52; N, 1.32; Zn, 8.23; P, 1.07; Mo, 36.71. Found (%): C, 24.13; H, 3.98; O, 24.33; N, 1.28; Zn, 8.65; P, 0.98; Mo, 36.88. ICP and elemental analyses were used to calculate the formula of PET-Z-POMOF. PXRD and FT-IR were employed to determine the hydrolysis efficiency of PET of the reaction, as described earlier.

The preparation process of PBT-Z-POMOF is similar to that of PET-Z-POMOF except that PET (0.064 g, 0.33 mmol) was replaced by PBT (0.10 g, 0.45 mmol). PXRD and FT-IR analysis were used to measure the consumption of PBT in the reaction, as indicated earlier.

Syntheses of PET-VMOP-11 and PBT-VMOP-11

A mixture of $\text{VOSO}_4 \cdot \text{H}_2\text{O}$ (0.15 g, 0.70 mmol) and PET (0.10 g, 0.52 mmol) was added into 2 mL N,N-diethylformamide (DEF) and 1 mL CH_3OH . The mixed solution was sealed in a 15 mL Teflon-lined stainless steel autoclave tubes and heated at 180 °C for 48 h. After temperature cooled to room temperature, the remained PET was separated by handpicking and flotation, and the obtained yellowish-brown crystals were washed with DEF and ethanol for three times. PXRD and FT-IR tests were employed to determine the consumption of PET in the reaction. The FT-IR peaks are listed as follows (KBr, cm⁻¹): 2815 (w), 1750 (s), 1560 (s), 1402 (s), 1250 (s), 1200 (w), 1153 (w), 1100 (w), 1080 (m), 960 (w), 803 (m), 782 (m), 740 (s), 650 (s), 450 (s). Anal. Calcd (%) for $\text{C}_{126}\text{H}_{250}\text{N}_{10}\text{O}_{102}\text{S}_4\text{V}_{24}$: C, 30.82; H, 5.85; O, 33.4; N, 2.58; S, 2.62; V, 25.05. Found (%): C, 31.45; H, 5.04; O, 32.86; N, 2.36; S, 2.72; V, 24.88. ICP and elemental analyses were used to calculate the formula of PET-VMOP-11.

The preparation process of PBT-VMOP-11 was similar to that of PET-VMOP-11 except that PET (0.10 g, 0.52 mmol)

was replaced by PBT (0.10 g, 0.45 mmol). The PXRD and FT-IR tests were repeated for the determination of PBT consumption in the reaction.

Results and Discussion

One-pot conversion from plastics to POMOFs

One-pot POMs-based hydrolysis method for the syntheses of POMOFs was performed as follows. With the addition of POMs in the system, the waste polyester plastics were hydrolyzed spontaneously and fabricated with POMs to generate POMOFs. Specifically, the conversion from PET into POMOFs involved adding POM into the system with plastic pellets and conducting the reaction under hydrothermal conditions. For instance, with the addition of $\text{Ni}_6(\text{OH})_3(\text{H}_2\text{O})_6(\text{en})_3(\text{PW}_9\text{O}_{34})$ (Ni_6PW_9) as both hydrolysis agent and construction unit, Ni_6PW_9 -based POMOF (Ni-POMOF), for PET incorporation via the hydrolytic conversion to generate PET derivative of Ni-POMOF, denoted as PET-Ni-POMOF, while the PBT conversion by Ni-POMOF was denoted as PBT-Ni-POMOF, with an achievement of >95% PET and PBT hydrolysis efficiency, respectively, proven by powder X-ray diffraction (PXRD) and FT-IR tests (Figure 2b; Supporting Information Figure S2 and Table S1). In the secondary building unit (SBU) of Ni-POMOF, two Ni_6PW_9 clusters were connected with Ni-O(W) bond. The SBUs of Ni-POMOF were connected by four H_2BDC ligands to form a two-dimensional (2D) layer.³¹ In the 2D layer, six SBUs and six H_2BDC ligands assembled to generate a giant parallelogram-shaped ring with a size of $\sim 2.7 \times 3.8 \text{ nm}^2$ (measured between opposite atoms) (Figure 2a; Supporting Information Figure S1). PBT, another kind of polyester plastic, were also directly converted into PBT-Ni-POMOF under similar optimized conditions proved by PXRD and FT-IR tests (Figure 2b; Supporting Information Figure S3 and Table S1). Further, FT-IR and PXRD tests were conducted to determine the possibility of residual plastics in the obtained samples. Our results revealed no detectable plastic residues, compared with the raw PET or PBT plastic sample controls (Supporting Information Figures S2 and S3). Inductively coupled plasma (ICP) and elemental analyses revealed that the calculated formula for the representative conversion product, PET-Ni-POMOF, was $[\text{Ni}_6(\text{OH})_3\text{PW}_9\text{O}_{34}]_2(\text{BDC})_{1.5}[\text{Ni}(\text{OH})_2](\text{en})_7(\text{H}_2\text{O})_7$.

Notably, based on our calculation on the average market price in 2018, the cost of the PET hydrolysis reaction is even lower than that of H_2BDC (Supporting Information Table S2). Thus, our current reported method is highly desirable in replacing chemical reactions, which directly utilizes H_2BDC as the ligand source, and therefore, holds a great promise as an alternative reaction in waste-plastic treatment.

Typically, the hydrolysis of polyester plastics is an energy- and cost-consuming process. Accordingly, the reaction conditions need to be well-optimized for economically and energetically feasible target. We systematically explored the best reaction conditions for the synthesis procedures by examining various factors such as POM amount, temperature, and reaction time, while using the PET conversion by Ni-POMOF as the model reaction. We investigated the effect of POMs on the hydrolysis efficiency by varying the amounts of Ni_6PW_9 from 0 to 0.14 mmol, under fixed experimental conditions (Supporting Information Figure S4). Our results showed that, as the concentration of Ni_6PW_9 increased, the hydrolysis efficiency of PET reached a peak at $\sim 97\%$ efficiency at 0.082 mmol. Afterward, the hydrolysis efficiency was sustained at a maximum of $\sim 97\%$ with further increase in PET concentration up to 0.14 mmol, indicating the optimal amount of PET was 0.082 mmol for the hydrolysis reaction.

Additionally, varying temperatures were tested during the reaction. When the temperature was set at 100°C , only 6.8% hydrolysis efficiency was achieved (Supporting Information Figure S5). With an enhancement of temperature, the hydrolysis efficiency simultaneously increased, reaching a maximum at 180°C , with 97% efficiency, after which there was no dramatic increase in efficiency (98%) as the temperature was increased further to 200°C (Supporting Information Figure S5). Hence, by considering the energy consumption, the optimal temperature under the reaction conditions was 180°C . Moreover, a parallel experiment was carried out by varying the reaction time, under the same experimental conditions. As shown in Supporting Information Figure S6, the optimal reaction time for maximal hydrolysis efficiency was 72 h.

Besides, other acidic or basic systems like HF, HCl, and NaOH with similar mole amount were used to replace POMs. The detected plastic hydrolysis efficiency of HF, HCl, and NaOH was found to be much lower than that of Ni_6PW_9 , which indicated the superiority of POMs in the direct conversion of PET or PBT into Ni-POMOF (Supporting Information Figure S7).

To study the versatility of the protocol, we successfully applied two other types of POM systems [i.e., polyoxomolybdate ($\text{Zn}_4\text{PMo}_{12}$, stands for $[\text{PMo}^{\text{V}}_8\text{Mo}^{\text{VI}}_4\text{O}_{36}(\text{OH})_4\text{Zn}_4]^{+}$) and polyoxovanadate (V_6S , $[\text{V}^{\text{IV}}_6\text{O}_6(\text{OCH}_3)_9(\text{SO}_4)(\text{COO})_3]^{2-}$)] to generate POMOFs (i.e., Z-POMOF and VMOP-11) in the conversion of polyester plastics (i.e., PET and PBT) under our established optimized conditions, proven by PXRD and FT-IR tests (Supporting Information Figure S2b). Z-POMOF is a three-dimensional (3D) POMOF.³² In its structure, four $\text{Zn}_4\text{PMo}_{12}$ clusters coordinated with six BDC ligands to construct the basic unit and further assembled to generate the 3D topology (Figure 2a, Supporting Information Figure S1b). The hydrolysis efficiency values of the conversion from PET and PBT incorporation into Z-POMOF were

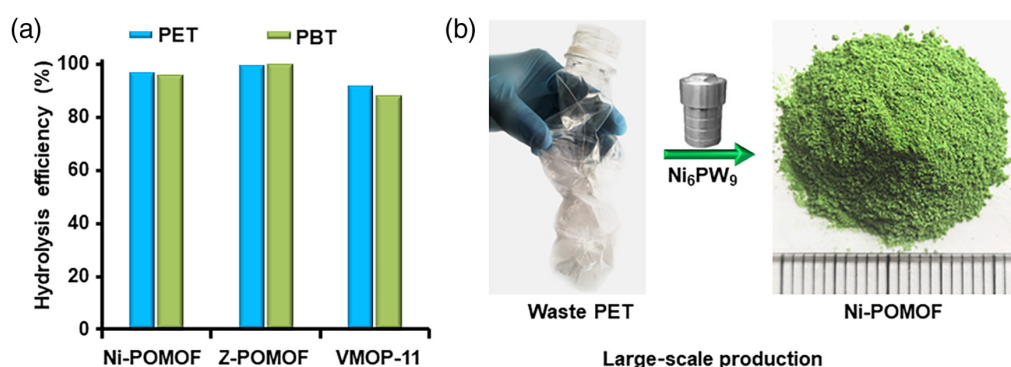


Figure 3 | Hydrolysis efficiency and scale-up production of POMOFs. (a) Hydrolysis efficiency from PET or PBT conversion into various POMOFs (the reported values are well-optimized ones). (b) The image of the large-scale production from waste PET into Ni-POMOF.

92% and 88%, respectively (Figure 3a), and based on the ICP and elemental analyses, the calculated formula for the representative conversion product, PET-Z-POMOF, was $[\text{TBA}]_3[\text{PMo}^{\text{V}}_8\text{Mo}^{\text{VI}}_4\text{O}_{36}(\text{OH})_4\text{Zn}_4(\text{BDC})_2]2\text{H}_2\text{O}$.

Furthermore, we repeated the hydrolysis experiment under similar optimized conditions, using a mixture of $\text{VOSO}_4\cdot\text{H}_2\text{O}$ and PET or PBT to generate PET-VMOP-11 and PBT-VMOP-11, respectively. We determined VMOP-11 as a metal-organic tetrahedral with tetrahedral topology, in which (V_6S) clusters served as the vertexes and H_2BDC ligands as the edges (Figure 2a; Supporting Information Figure S1c).³³ Notably, PXRD and FT-IR tests revealed 100% hydrolysis efficiency for both PET and PBT into VMOP-11 (Figure 3a). Based on the ICP and elemental analyses, the calculated formula for the representative conversion product, PET-VMOP-11, was $[\text{NH}_2\text{Et}_2]_8[\text{V}_6\text{O}_6(\text{OCH}_3)_9(\text{SO}_4)_4(\text{BDC})_6(\text{DEF})_2]$.

Finally, we carried out the conversion of polyester plastics using POMs as the hydrolysis agents. Our results demonstrated that the POMs were separately connected by the plastic hydrolyzed product (a type of rigid ligand called H_2BDC) to generate robust POMOFs.²³ Taking PET-Ni-POMOF, for example, we found that it exhibited high chemical and thermal stability. The structural integrity of PET-Ni-POMOF remained unchanged in common organic solvents, including aniline, chloroform, and tetrahydrofuran, and water heated to 100 °C for more than 3 days, as revealed by PXRD tests (Supporting Information Figure S8). Besides, the generated PET-Ni-POMOF was tolerant to harsh acidic or basic conditions with a wide pH range from 4 to 10 for more than 3 days, which is comparable to stable MOFs like UiO-66 (Supporting Information Figure S8).³⁴ Likewise, the PET-Ni-POMOF was stable at temperatures as high as 300 °C under atmospheric N_2 , certified by variable PXRDs temperatures (Supporting Information Figure S9) and thermogravimetric analyses (Supporting Information Figure S10). Noteworthy, this method could be scaled-up easily: When the reaction reagents were expanded 15 times, large amounts of

PET-Ni-POMOF and PET-VMOP-11 with high hydrolysis efficiency (>95%) were obtained successfully, as proven by PXRD tests (Figure 3b; Supporting Information Figures S11 and S12).

Characterization of the obtained POMOFs

Considering combining high stability with the possibility of mass production together, we examined if the POMOFs fabricated as a result of our hydrolysis reaction might serve as powerful catalysts. N_2 sorption test of PET-Ni-POMOF was conducted to evaluate porosity, and it exhibited an S_{BET} of $51 \text{ m}^2 \text{ g}^{-1}$, close to that of BDC-Ni-POMOF ($62 \text{ m}^2 \text{ g}^{-1}$), made via direct synthesis with terephthalic acid (Supporting Information Figure S14).³¹ Ni-POMOF is a 2D POMOF constructed from Ni_6PW_9 and BDC. Its pore size was $\sim 2.7 \times 3.8 \text{ nm}^2$, which matched well with the pore-size distribution of $\sim 3.1 \text{ nm}$ for Ni-POMOF and BDC-Ni-POMOF (Supporting Information Figures S13 and S14). More so, CO_2 adsorption and NH_3 -temperature-programmed desorption (NH_3 -TPD) tests were conducted to evaluate the porosity and catalytic sites of the obtained POMOFs. For the CO_2 adsorption evaluation, the adsorption capacity of PET-Ni-POMOF ranged from 3.70 to 2.74 wt % at temperatures between 273 and 298 K, respectively (Supporting Information Figure S15). Besides, the NH_3 -TPD tests conducted showed some exposed catalytic sites, consistent with the observation made by Chen et al.³⁵ with the cerium (Ce)-MOF (BIT-58), of increased acidic site. In our case, the amount of acid site calculated for PET-Ni-POMOF was 0.95 mmol g^{-1} , within a temperature range of 50–300 °C (Supporting Information Figure S16), reflecting its thermal stability. Collectively, these findings indicate that Ni-POMOF exhibits a promising catalytic role.

Based on the above-mentioned Ni-POMOF properties, we set out to explore the catalysis performances of Ni-POMOF, focused on the cycloaddition of epoxides and CO_2 into cyclic carbonates, as a means of reducing

pollution associated with polymer production, as well as promoting usage of carbon dioxide. The products of this catalysis were important precursors of polycarbonate plastics, commonly used in the fabrication of commercial products like compact discs, DVDs, or cockpit canopy of battleplanes.^{36,37} We tested our hypothesis of successful conversion of waste polyester plastic as powerful catalysts to efficiently fabricate other types of plastic derivatives by the conversion of epoxides into cyclic carbonates. In previous reports, the process had been conducted typically under high-pressure and by the use of flue mixed gas, generated from coal-fired power plants.³⁸ In contrast, we investigated the cycloaddition of epoxides under less stringent reaction conditions, applying normal pressure and simulated flue gas from coal-fired power plant that captures pure CO₂ to explore the fixation of the CO₂ into cyclic carbonates, as follows:

First, PET-Ni-POMOF was applied as the catalyst to study the cycloaddition of epichlorohydrin with CO₂ under pure CO₂ and normal pressure (1 atm) conditions without the addition of solvents. Ni-POMOF displayed 99.3% conversion efficiency and 97.5% selectivity in the catalysis of the cycloaddition of epichlorohydrin with CO₂ into 4-chloromethyl-1,3-dioxolan-2-one (Figure 4a and Supporting Information Table S3). The turnover number was calculated to be 244. In contrast, H₂BDC and POM tested as comparisons under similar catalysis

conditions yielded 69.3% and 89.6%, respectively (Supporting Information Figure S17). We discovered that the structural integrity of PET-Ni-POMOF remained unchanged after the catalysis, as revealed by PXRD, FT-IR, and X-ray photoelectron spectroscopy analyses (Supporting Information Figures S18 and S19). As showed in Figure 4b, the performance of PET-Ni-POMOF was superior to most of reported MOFs under normal pressure in the catalysis of cycloaddition of epichlorohydrin with CO₂ (for the detailed performance data of various MOFs, see Supporting Information Table S6).³⁹⁻⁴²

Second, a series of epoxide substrates were tested for the syntheses of their corresponding cyclic carbonates via CO₂ fixation (Figure 4a). The yields varied from 10.4% to 96.8% as detected both by gas chromatography and gas chromatography-mass spectrometry (Supporting Information Figures S20 and S21 and Supporting Information Table S3). Remarkably, the conversion process of (S)-glycidyl phenyl ether to the cyclic carbonate via CO₂ fixation yielded 98.5% conversion efficiency and 98.2% selectivity. Surprisingly, for the conversion of cyclohexene oxide through CO₂ fixation into aliphatic polycarbonates yielded only 10.4%, which, presumably, was attributable to the effect of the steric hindrance of the alkyl structures inhibiting the proximity of the epoxide to the reactive sites (Figure 4a).⁴³

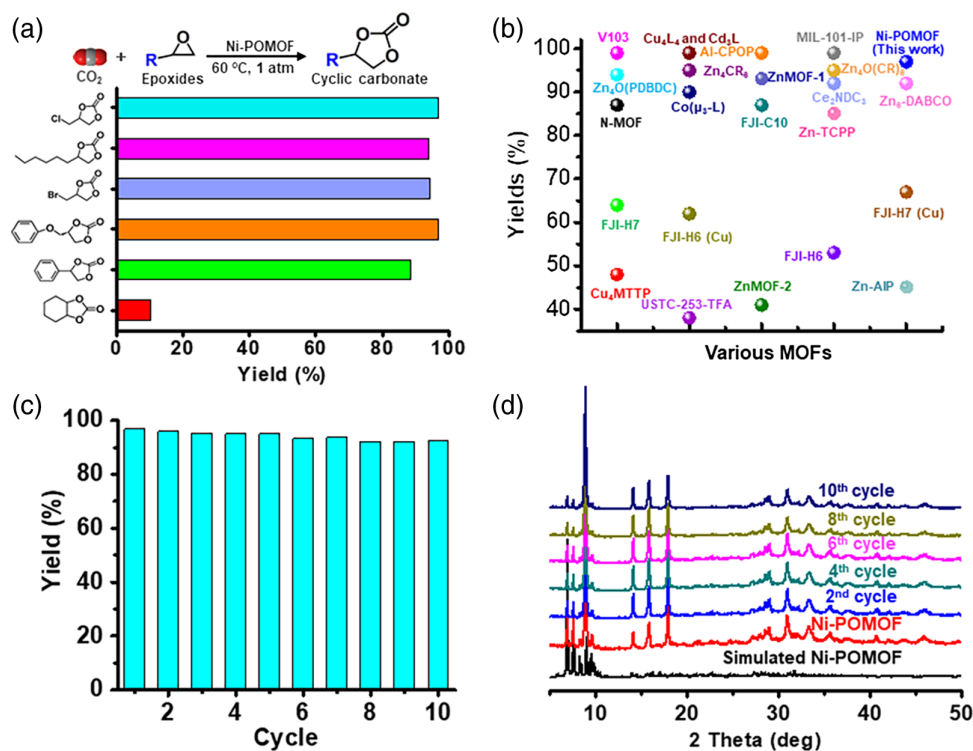


Figure 4 | Catalysis and recycle performances of PET-Ni-POMOF. (a) The catalysis performances of PET-Ni-POMOF in the conversion of epoxides into cyclic carbonates. (b) A representation of performances of various MOFs reported for the cycloaddition of epichlorohydrin with CO₂ under normal pressure. (c) The recycle performances of PET-Ni-POMOF. (d) The PXRD patterns of PET-Ni-POMOF in recycling experiments.

Third, as recyclability is an essential property to evaluate the durability of a catalyst, we conducted recycling experiments by applying the CO₂ into epichlorohydrin cycloaddition as a model reaction. The FT-IR spectra and PXRD patterns of the recovered PET-Ni-POMOF were identical to those freshly prepared (Supporting Information Figure S18). In addition, the recovered PET-Ni-POMOF could be reused in repetitive reactions with negligible loss of its high catalytic performance, even after 10 cycles [yields: 96.7% (first run), 96.0% (second run), 95.1% (forth run), 93.2% (sixth run), 92.1% (eighth run), and 92.4% (10th run)] (Figure 4c and Supporting Information Table S4). Notwithstanding, after 10 catalysis cycles, the structural integrity of PET-Ni-POMOF remained intact, proven by FT-IR spectra and PXRD tests (Figure 4d and Supporting Information Figure S22). Moreover, leaching tests conducted for further evaluation demonstrated profound stability of PET-Ni-POMOF. Also, negligible leaching elements (i.e., Ni and W) were detected (<0.02 mg L⁻¹) after 10 reaction cycles. Furthermore, CO₂ adsorption property of PET-Ni-POMOF tested after 10 cycles showed a 3.70 wt % adsorption capacity, equivalent to the CO₂ adsorption property (3.71 wt %) recorded before the catalytic cycles (Supporting Information Figure S23), confirming a full recovery of catalytic performance of the PET-Ni-POMOF, post 10 catalytic cycles.

Fourth, apart from the catalysis condition conducted under pure CO₂, the use of mixed gases was also tested. Generally, the flue gas (released at a total pressure of ~1 atm) is generated from coal-fired power plant containing 15–16% CO₂, 73–77% N₂, 5–7% H₂O, 3–4% O₂, and a small amount of acid gas.^{44,45} Mixed N₂/CO₂ gas, with a ratio of ~0.85/0.15 at 1 atm, simulates the flue gas from coal-fired power plant, was applied as the CO₂ source. The experiment was conducted under similar experimental conditions at normal atmospheric pressure, with PET-Ni-POMOF displaying 84.6%, 78.5%, and 76.3% yields in cycloaddition reactions with the epichlorohydrin, styrene oxide, and (S)-glycidyl phenyl ether, respectively (Supporting Information Table S5). Undoubtedly, these presented yields are slightly lower, compared with those obtained with the reactions performed under pure CO₂ conditions at normal atmospheric pressure, leading us to infer that, a combination of high chemical stability with high reaction efficiency, renders PET-Ni-POMOF, a favorable candidate in practical catalysis applications.

Finally, we explored this eco-friendly, catalyst, which could be regenerated and recycled multiple times to minimize waste production (green catalyst) in other catalysis reactions. Based on reported pieces of literature, Knoevenagel condensation, nucleophilic addition of an active hydrogen compound to a carbonyl group, followed by a dehydration reaction, has a high potential for the syntheses of drug intermediates.⁴⁶ The reaction

proceeds with a critical carbon–carbon bond formation for the manufacture α,β -unsaturated carbonyl compounds, which are pivotal intermediates for the production of pharmaceuticals, fine chemicals, and others.⁴⁷ By applying PET-Ni-POMOF as the catalyst, 99% conversion, and 98% selectivity was achieved for the Knoevenagel condensation of benzaldehyde and propylene under none-solvent conditions at 40 °C for 3 h (Supporting Information Figure S24). After the catalysis, the inert structure of PET-Ni-POMOF remained intact, compared with the simulated Ni-POMOF, as revealed by PXRD patterns (Supporting Information Figure 25b). In addition, the PET-Ni-POMOF exhibits high performance in recycling experiments. After three catalysis cycles, the yield was sustained at ~95%, and the topology of PET-Ni-POMOF was well-maintained, as proven by PXRD analysis (Supporting Information Figure S25), again confirming the potential of PET-Ni-POMOFs to serve as efficient and durable catalysts.

Conclusions

Our current study presents a general and versatile POM-based protocol of hydrolytic degradation of plastic into highly valuable, recyclable, and biocompatible polymers via one-pot syntheses of POMOFs. This protocol could be applied to diverse kinds of plastics (i.e., PET and PBT) and various POM systems [e.g., polytungstate (Ni₆PW₉), polyoxomolybdate (Zn₄PMo₁₂), and polyoxovanadate (V₆S)] to generate POMOFs (i.e., Ni-POMOF, Z-POMOF, and VMOP-11) with 100% or close to 100% hydrolysis efficiency. In this method, we showed that POMs could act both as hydrolysis agents and construction units under reduced or absence of acidic or basic conditions. POMOFs obtained, from such an environmental-friendly approach could efficiently catalyze the synthesis of cyclic carbonate compounds (precursors of polycarbonate); thus, they could be used to achieve the conversion from one type of plastic to more regeneratable and biodegradable derivatives. Moreover, our versatile method could be easily upscaled, and hence, holds great promise in industrial production. Accordingly, this effective protocol is favorable in the conversion of waste polyester plastics into value-added products, including industrial-scale applications in energy storage and conversion, electrochemical energy conversion in rechargeable batteries, used for portable electronic devices, as well as photo (electro) catalytic and electroanalytical properties; thus, shedding light on the development of economically and environmentally-friendly plastic-recycle techniques.

Supporting Information

Supporting information is available.

Conflicts of Interest

There are no conflicts to declare.

Author Contributions

Y.-J.C., X.H., Y.C., and Y.-Q.L. conceived the idea. Y.-J.C., X.H., Y.C.S.L., and Y.-Q.L. designed the experiments, collected and analyzed the data. Y.-R.W., H.Z., L.Z., H.Z., and R.Y. assisted with the experiments and characterizations. Y.C. and Y.-J.C. wrote the manuscript. All authors discussed the results and commented on the manuscript.

Acknowledgments

This work was supported financially by National Nature Science Foundation of China (NSFC) (nos. 21622104, 21701085, 21871125, 21871141, 21871142, and 21901122); The National Science Foundation (NSF) of Jiangsu Province of China (no. BK20171032); the Natural Science Research of Jiangsu Higher Education Institutions of China (nos. 17KJB150025 and 19KJB150011); and Project funded by China Postdoctoral Science Foundation (nos. 2018M630572 and 2019M651873); Priority Academic Program Development of Jiangsu Higher Education Institutions and the Foundation of Jiangsu Collaborative Innovation Center of Biomedical Functional Materials.

References

1. Thompson, R. Environment: A Journey on Plastic Seas. *Nature* **2017**, *547*, 278–279.
2. The Future of Plastic. *Nat. Commun.* **2018**, *9*, 2157.
3. Welden, N. A.; Cowie, P. R. Degradation of Common Polymer Ropes in a Sublittoral Marine Environment. *Mar. Pollut. Bull.* **2017**, *118*, 248–253.
4. Geyer, R.; Jambeck, J. R.; Law, K. L. Production, Use, and Fate of All Plastics Ever Made. *Sci. Adv.* **2017**, *3*, e1700782.
5. Joo, S.; Cho, I. J.; Seo, H.; et al. Structural Insight into Molecular Mechanism of Poly(ethylene terephthalate) Degradation. *Nat. Commun.* **2018**, *9*, 382.
6. Welle, F. Twenty Years of PET Bottle to Bottle Recycling—An Overview. *Resour. Conserv. Recy.* **2011**, *55*, 865–875.
7. Chiu, S. J.; Wu, Y. S. A Comparative Study on Thermal and Catalytic Degradation of Polybutylene Terephthalate. *J. Anal. Appl. Pyrol.* **2009**, *86*, 22–27.
8. Tsintzou, G. P.; Achilias, D. S. Chemical Recycling of Polycarbonate Based Wastes Using Alkaline Hydrolysis Under Microwave Irradiation. *Waste Biomass. Valori.* **2013**, *4*, 3–7.
9. Karayannidis, G. P.; Chatziavgoustis, A. P.; Achilias, D. S. Poly(ethylene terephthalate) Recycling and Recovery of Pure Terephthalic Acid by Alkaline Hydrolysis. *Adv. Polym. Tech.* **2002**, *21*, 250–259.
10. Yoshioka, T.; Motoki, T.; Okuwaki, A. Kinetics of Hydrolysis of Poly(Ethylene Terephthalate) Powder in Sulfuric Acid by a Modified Shrinking-Core Model. *Ind. Eng. Chem. Res.* **2001**, *40*, 75–79.
11. Al-Sabagh, A. M.; Yehia, F. Z.; Eshaq, G.; et al. Greener Routes for Recycling of Polyethylene Terephthalate. *Egypt. J. Pet.* **2016**, *25*, 53–64.
12. Goje, A. S.; Chauhan, Y. P.; Mishra, S. Chemical Recycling and Kinetics of Aqueous Alkaline Depolymerization of Poly(Butylene Terephthalate) Waste. *Chem. Eng. Technol.* **2010**, *27*, 790–799.
13. Li, H.; Eddaoudi, M.; O’Keeffe, M.; et al. Design and Synthesis of an Exceptionally Stable and Highly Porous Metal-Organic Framework. *Nature* **1999**, *402*, 276–279.
14. Kitaura, R.; Kitagawa, S.; Kubota, Y.; et al. Formation of a One-Dimensional Array of Oxygen in a Microporous Metal-Organic Solid. *Science* **2002**, *298*, 2358–2361.
15. Férey, G.; Mellot-Draznieks, C.; Serre, C.; et al. A Chromium Terephthalate-Based Solid with Unusually Large Pore Volumes and Surface Area. *Science* **2005**, *309*, 2040–2042.
16. Shekhah, O.; Belmabkhout, Y.; Chen, Z.; et al. Made-to-Order Metal-Organic Frameworks for Trace Carbon Dioxide Removal and Air Capture. *Nat. Commun.* **2014**, *5*, 4228.
17. Liao, P. Q.; Zhu, A. X.; Zhang, W. X.; et al. Self-Catalysed Aerobic Oxidization of Organic Linker in Porous Crystal for On-Demand Regulation of Sorption Behaviours. *Nat. Commun.* **2015**, *6*, 6350.
18. Yuan, S.; Feng, L.; Wang, K.; et al. Stable Metal-Organic Frameworks: Design, Synthesis, and Applications. *Adv. Mater.* **2018**, *30*, 1704303.
19. Dhakshinamoorthy, A.; Asiri, A. M.; Garcia, H. Metal-Organic Framework (MOF) Compounds: Photocatalysts for Redox Reactions and Solar Fuel Production. *Angew. Chem. Int. Ed.* **2016**, *55*, 5414–5418.
20. Nohra, B.; El Moll, H.; Rodriguez Albelo, L. M.; et al. Polyoxometalate-Based Metal-Organic Frameworks (POMOFs): Structural Trends, Energetics, and High Electrocatalytic Efficiency for Hydrogen Evolution Reaction. *J. Am. Chem. Soc.* **2011**, *133*, 13363–13374.
21. Du, D. Y.; Qin, J. S.; Li, S. L.; et al. Recent Advances in Porous Polyoxometalate-Based Metal-Organic Framework Materials. *Chem. Soc. Rev.* **2014**, *43*, 4615–4632.
22. Wales, D. J.; Cao, Q.; Kastner, K.; et al. 3D-Printable Photochromic Molecular Materials for Reversible Information Storage. *Adv. Mater.* **2018**, *30*, 1800159.
23. Huang, R. W.; Wei, Y. S.; Dong, X. Y.; et al. Hypersensitive Dual-Function Luminescence Switching of a Silver-Chalcogenolate Cluster-Based Metal-Organic Framework. *Nat. Chem.* **2017**, *9*, 689–697.
24. Deleu, W. P. R.; Stassen, I.; Jonckheere, D.; et al. Waste Pet (Bottles) as a Resource or Substrate for MOF Synthesis. *J. Mater. Chem. A.* **2016**, *4*, 9519–9525.
25. Ren, J.; Dyosiba, X.; Musyoka, N. M.; et al. Green Synthesis of Chromium-Based Metal-Organic Framework (Cr-MOF) from Waste Polyethylene Terephthalate (PET) Bottles for Hydrogen Storage Applications. *Int. J. Hydrogen Energy* **2016**, *41*, 18141–18146.
26. Manju, Roy, P. K.; Ramanan, A.; et al. Post Consumer PET Waste as Potential Feedstock for Metal Organic Frameworks. *Mater. Lett.* **2013**, *106*, 390–392.

27. Singh, S.; Sharma, S.; Umar, A.; et al. Nanocuboidal-Shaped Zirconium Based Metal Organic Framework (UIO-66) for the Enhanced Adsorptive Removal of Nonsteroidal Anti-Inflammatory Drug, Ketorolac Tromethamine, from Aqueous Phase. *New J. Chem.* **2017**, *42*, 1921–1930.
28. Dyosiba, X.; Ren, J.; Musyoka, N. M.; et al. Preparation of Value-Added Metal-Organic Frameworks (MOFs) Using Waste Pet Bottles as Source of Acid Linker. *Sustainable Mater. Technol.* **2016**, *10*, 10–13.
29. Raja, D. S.; Pan, C. C.; Chen, C. W.; et al. Synthesis of Mixed Ligand and Pillared Paddlewheel MOFs Using Waste Polyethylene Terephthalate Material as Sustainable Ligand Source. *Micropor Mesopor Mater.* **2016**, *231*, 186–191.
30. Lo, S. H.; Raja, D. S.; Chen, C. W.; et al. Waste Polyethylene Terephthalate (PET) Materials as Sustainable Precursors for the Synthesis of Nanoporous MOFs, MIL-47, MIL-53(Cr, Al, Ga) and MIL-101(Cr). *Dalton Trans.* **2016**, *45*, 9565–9573.
31. Zheng, S. T.; Zhang, J.; Yang, G. Y. Designed Synthesis of POM–Organic Frameworks from $\{\text{Ni}_6\text{PW}_9\}$ Building Blocks Under Hydrothermal Conditions. *Angew. Chem. Int. Ed.* **2008**, *47*, 3909–3913.
32. Rodriguez-Albelo, L. M.; Ruiz-Salvador, A. R.; Sampieri, A. et al. Zeolitic Polyoxometalate-Based Metal-Organic Frameworks (Z-POMOFs): Computational Evaluation of Hypothetical Polymorphs and the Successful Targeted Synthesis of the Redox-Active Z-POMOF₁. *J. Am. Chem. Soc.* **2009**, *131*, 16078–16087.
33. Zhang, Y. T.; Wang, X. L.; Li, S. B.; et al. Anderson-Like Alkoxo-Polyoxovanadate Clusters Serving as Unprecedented Second Building Units to Construct Metal-Organic Polyhedra. *Chem. Commun.* **2016**, *52*, 9632–9635.
34. Kandiah, M.; Nilsen, M. H.; Usseglio, S.; et al. Synthesis and Stability of Tagged UIO-66 Zr-MOFs. *Chem. Mater.* **2010**, *22*, 6632–6640.
35. Chen, Y.; Zhang, S.; Chen, F.; et al. Defects Engineering of Highly Stable Lanthanide Metal-Organic Frameworks by Particle Modulation for Coating Catalysis. *J. Mater. Chem. A.* **2017**, *6*, 342–348.
36. Ji, G.; Yang, Z.; Zhang, H.; et al. Hierarchically Mesoporous o-Hydroxyazobenzene Polymers: Synthesis and Their Applications in CO₂ Capture and Conversion. *Angew. Chem. Int. Ed.* **2016**, *55*, 9685–9689.
37. Feng, D.; Chung, W. C.; Wei, Z.; et al. Construction of Ultrastable Porphyrin Zr Metal-Organic Frameworks Through Linker Elimination. *J. Am. Chem. Soc.* **2013**, *135*, 17105–17110.
38. Liang, L.; Liu, C.; Jiang, F.; et al. Carbon Dioxide Capture and Conversion by an Acid-Base Resistant Metal-Organic Framework. *Nat. Commun.* **2017**, *8*, 1233.
39. Li, P. Z.; Wang, X. J.; Liu, J.; et al. A Triazole-Containing Metal-Organic Framework as a Highly Effective and Substrate Size-Dependent Catalyst for CO₂ Conversion. *J. Am. Chem. Soc.* **2016**, *138*, 2142–2145.
40. Zheng, J.; Wu, M.; Jiang, F.; et al. Stable Porphyrin Zr and Hf Metal-Organic Frameworks Featuring 2.5 nm Cages: High Surface Areas, SCSC Transformations and Catalyses. *Chem. Sci.* **2015**, *6*, 3466–3470.
41. Liang, J.; Chen, R. P.; Wang, X. Y.; et al. Postsynthetic Ionization of an Imidazole-Containing Metal-Organic Framework for the Cycloaddition of Carbon Dioxide and Epoxides. *Chem. Sci.* **2017**, *8*, 1570–1575.
42. Aguila, B.; Sun, Q.; Wang, X.; et al. Lower Activation Energy for Catalytic Reactions Through Host-Guest Cooperation Within Metal-Organic Frameworks. *Angew. Chem. Int. Ed.* **2018**, *57*, 10107–10111.
43. Huang, X.; Chen, Y.; Lin, Z.; et al. Zn-BTC MOFs with Active Metal Sites Synthesized via a Structure-Directing Approach for Highly Efficient Carbon Conversion. *Chem. Commun.* **2014**, *50*, 2624–2627.
44. Wilmer, C. E.; Farha, O. K.; Bae, Y. S.; et al. Structure-Property Relationships of Porous Materials for Carbon Dioxide Separation and Capture. *Energ. Environ. Sci.* **2012**, *5*, 9849–9856.
45. Mason, J. A.; McDonald, T. M.; Bae, T. H.; et al. Application of a High-Throughput Analyzer in Evaluating Solid Adsorbents for Post-Combustion Carbon Capture via Multicomponent Adsorption of CO₂, N₂, and H₂O. *J. Am. Chem. Soc.* **2015**, *137*, 4787–4803.
46. Li, W.; Fedosov, S. N.; Tan, T.; et al. Kinetic Insights of DNA/RNA Segment Salts Catalyzed Knoevenagel Condensation Reaction. *ACS Catal.* **2014**, *4*, 3294–3300.
47. Ansari, M. B.; Jin, H.; Parvin, M. N.; et al. Mesoporous Carbon Nitride as a Metal-Free Base Catalyst in the Microwave Assisted Knoevenagel Condensation of Ethyl Cyanoacetate with Aromatic Aldehydes. *Catal. Today* **2012**, *185*, 211–216.